Accepted Manuscript

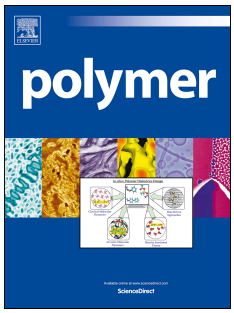

Latent curing of epoxy-thiol thermosets

Ali Osman Konuray, Xavier Fernández-Francos, Xavier Ramis

PII: S0032-3861(17)30329-4

DOI: 10.1016/j.polymer.2017.03.064

Reference: JPOL 19560

To appear in: *Polymer*

Received Date: 9 February 2017

Revised Date: 21 March 2017

Accepted Date: 24 March 2017

Please cite this article as: Konuray AO, Fernández-Francos X, Ramis X, Latent curing of epoxy-thiol thermosets, *Polymer* (2017), doi: 10.1016/j.polymer.2017.03.064.

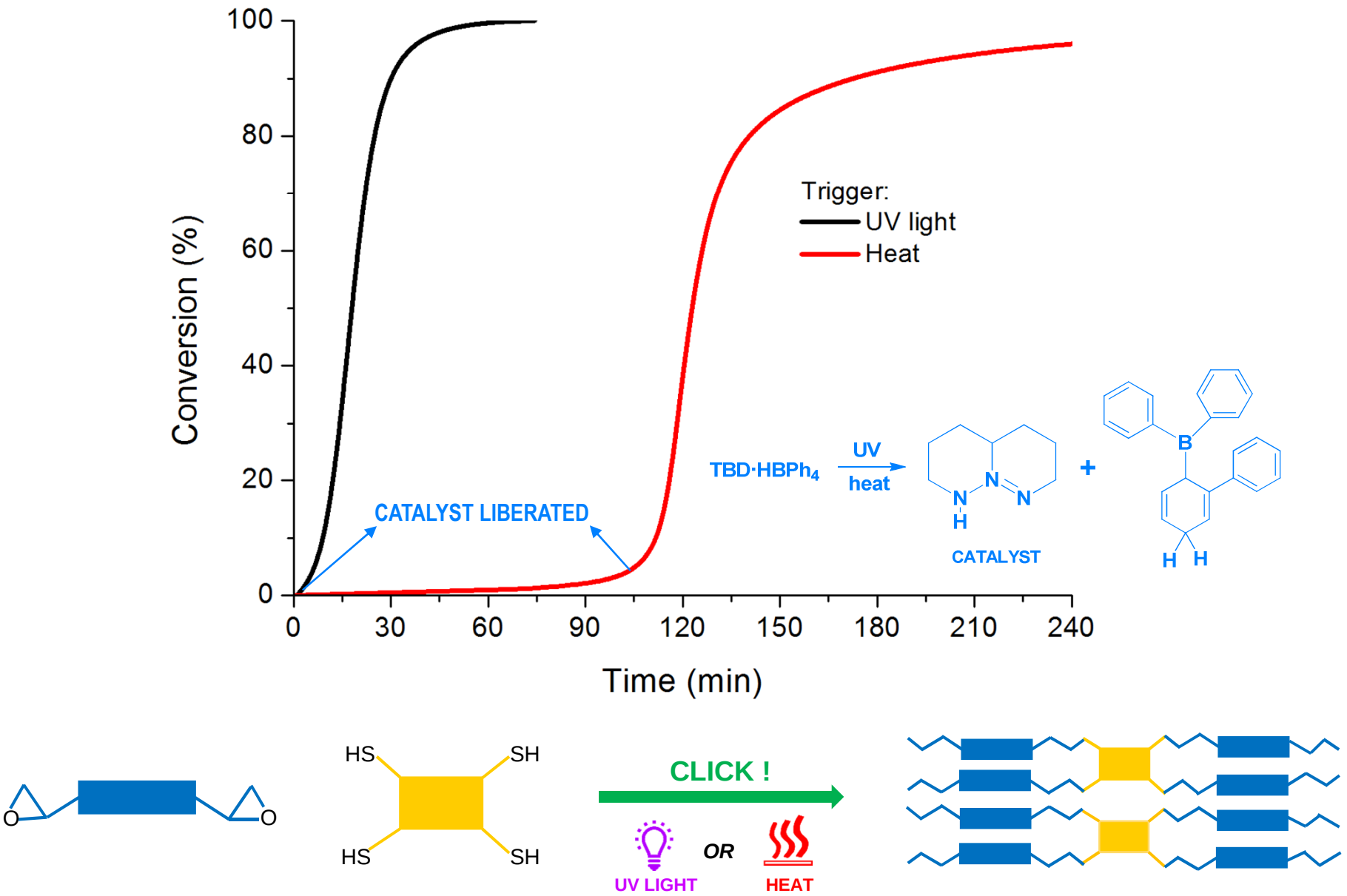
Conversion (%)
Time (min)
Trigger:
UV light
Heat
CATALYST LIBERATED
TBD·HBPh4
UV
heat
CATALYST
HS
SH
HS
SH
CLICK !
OR
UV LIGHT
HEAT

LATENT CURING OF EPOXY-THIOL THERMOSETS

Ali Osman Konuray*, Xavier Fernández-Francos, Xavier Ramis

Thermodynamics Laboratory, ETSEIB, Universitat Politècnica de Catalunya, Av. Diagonal 647, 08028 Barcelona, Spain

*Corresponding author

E-mail: osman.konuray@mmt.upc.edu

Phone: +34 934016593

Fax: +34 934017389

ABSTRACT

Epoxy-thiol curing is a click reaction which allows quantitative yield of the end products. The base-catalyzed reaction is rapid at low temperatures so it is most often desirable to harness reactivity by using latent catalysts. In this work, we used triazabicyclodecene tetraphenylborate (TBD·$HBPh_4$) as a photobase generator (PB). We activated the PB either thermally or by UV light and monitored reaction kinetics by DSC and FTIR methods. Depending on the catalytic system used, the rate of the thiol-epoxy reaction was ordered as follows: Neat base > UV activated PB > thermally activated PB > uncatalyzed system. A series of isothermal and non-isothermal DSC experiments were run on non-irradiated and irradiated samples in order to study the effect of PB content and UV irradiation duration on PB activation efficiency and latency / storage stability. The data from DSC were analyzed using model-free linear isoconversional methods to estimate kinetic parameters such as activation energies. In addition, the kinetics data for both activation methods were shown to be accurately represented by multi-term Kamal models. The storage stability of the systems were studied at room temperature and was shown to fit well to the predictions of the kinetic model.

Keywords: Epoxy-thiol, click reaction. curing kinetics, photobase, latency

1 Introduction

Epoxy resins are one of the most used polymeric resins due to their superior performance in many industrial applications. They can be formulated as two-pack systems with a wide selection of curing agents including amines, amides, phenols, carboxylic acids, anhydrides and thiols [1]. Epoxy-thiol systems have been studied relatively less, despite their advantages such as high yield of the curing reaction, superior mechanical properties of end products [2], and their numerous industrial uses such as adhesives, nanocomposites, shape-memory materials and biomedical materials [3,4].

The curing of epoxy resins by thiols proceeds through a click reaction which allows quantitative yield of the epoxy-thiol thermoset. Although the reaction can take place at elevated temperatures without requiring any catalyst, lower curing temperatures can be achieved by using base catalysts. In the base catalyzed epoxy-thiol reaction, the base helps generate thiolate anions by deprotonating thiols. In turn, the thiolate anions couple with the epoxide groups through a nucleophilic ring opening reaction. The resulting alcoholate anions are protonated either by the base catalyst or the thiol to yield the desired reaction products. The reaction exhibits auto-catalytic behavior due to the hydroxyl groups formed [4,5]. Consequently, any further kinetic study of this reaction must account for this effect. The reaction steps for the base-catalyzed reaction are shown in Scheme 1. An alternative reaction scheme involving the nucleophilic attack of the tertiary amine to the epoxy ring as initiation step was proposed by Loureiro et al. [6] which was found to be operative in the curing of thiol-epoxy formulations using a weak base such as 1-methylimidazole [7].

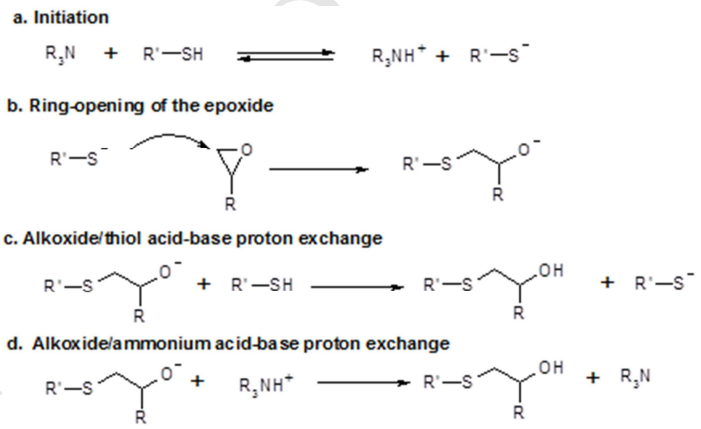

Scheme 1: Proposed curing mechanism for the base-catalyzed thiol-epoxy condensation.

Epoxy-thiol systems catalyzed by bases have fast initial curing rates which lead to undesirably short pot-lives. In order to prepare one-pack formulations, latent catalysts must be used. These catalysts, as the name implies, have latent activity which can only be initiated by external stimuli such as heat or irradiation. They allow storage stability and provide freedom to start the curing reaction whenever desired. In a recent paper, latent thiol-epoxy formulations were developed making use of encapsulated imidazole and urone catalysts that are activated upon heating [3]. Another feasible solution is the use of photobase generators (PB) [8–11]. A PB releases a catalytic base upon UV irradiation which, in turn, initiates the curing reaction. In our

work, we use triazabicyclodecene tetraphenylborate (TBD·$HBPh_4$) as a PB [12]. Upon photolysis, TBD·$HBPh_4$ releases triazabicyclodecene (TBD), a strong base, with a pKa of 20 in tetrahydrofuran and 26 in acetonitrile [13] that can be used in a variety of base-catalyzed processes. However, given their low quantum yield and the limited absorption range (below 300 nm wavelength), tetraphenylborate PBs are commonly used in combination with photosensitizers such as isopropylthioxane (ITX) [8,9] in order to extend the absorption range towards longer wavelengths, up to the visible light range.

However, tetraphenyl borate amine salts can also be used as latent thermal catalysts. For instance, Kim and Chun [14] used commercially available 2,4-ethylmetylimidazole tetraphenylborate as catalyst for the reaction between naphtol and their epoxy derivatives, which can be catalyzed by bases such as imidazoles [15]. Therefore, for base-catalyzed reactions, tetraphenylborate ammonium salts have a dual photo-latent and thermally latent character that can be triggered with UV-light under mild temperature conditions or thermally activated where UV irradiation is not possible. This is an interesting feature which is also present in cationic catalysts such as diaryliodonium salts [16,17].

In this paper we study the applicability of TBD·$HBPh_4$ as thermally-latent and photolatent base for the curing of thiol-epoxy formulations based on diglycidyl ether of Bisphenol-A and pentaerythrithol tetrakis(3-mercaptopropionate) as crosslinking agent. The curing kinetics are analyzed using differential scanning calorimetry (DSC) and Fourier-transform infrared spectroscopy (FTIR). Model-free isoconversional methods and model-fitting methods are used to derive the kinetic parameters of the UV-activated or thermally-activated process. The storage stability of the materials are also analyzed.

2 Experimental

2.1 Materials

DGEBA with an epoxy equivalent weight of 187 g/eq (DG187, Epikote 828, Hexion Speciality Chemicals B.V.) was dried under vacuum prior to use. Pentaerythritol tetrakis (3-mercaptopropionate) (S4), triazabicyclodecene (TBD) and sodium tetraphenylborate ($NaBPh_4$) were supplied by Aldrich and used as received. Methanol (MeOH) and chloroform ($CHCl_3$) were supplied by VWR and used as received. Isopropylthioxane (ITX) was supplied by Ciba Specialty Chemicals Inc. and used as received.

TBD·$HBPh_4$ (PB hereafter) was synthesized using the procedure outlined in Ref [13]. Firstly, TBD was solubilized in methanol (10 mmol in 10 mL MeOH) and slightly acidified with 36% HCl solution. $NaBPh_4$ was also solubilized in a small amount of MeOH and added with a slight excess to the acidified TBD solution. The formed salt was filtered, washed thoroughly with distilled water and MeOH, recrystallized from a 4:1 mixture of MeOH and $CHCl_3$, filtered and dried under mild heat and vacuum. To analyze its purity, its melting point was measured in a DSC thermal scan and was found to be identical to what is reported by Sun et al [12].

Curing samples were prepared in 5 mL vials in 1-2 gr batches using the following procedure: PB was weighed and added to DG187 and was kept under agitation at 110ºC for 15 minutes. With this mixing procedure, an optimum balance between dispersion quality and latency is achieved. The mixture was left to cool down to room temperature after which S4 was added in a stoichiometric amount. To avoid premature activation, ITX was added lastly. The mixture was stirred continuously until homogeneous and subsequently analyzed. The samples not planned for immediate analysis were kept in a freezer at -20ºC. We coded our epoxy-thiol mixtures as *PBx UVy*, where *x* is the PB content in phr and is either 0.5, 1 or 2, and *y* indicates the duration (in minutes) of prior UV irradiation. Coding was done as *PBx noUV* for samples who were not UV irradiated. On the basis of previous works [9] the amount of ITX used was half the amount of PB in all formulations. The structures of the reagents used are shown in Scheme 2.

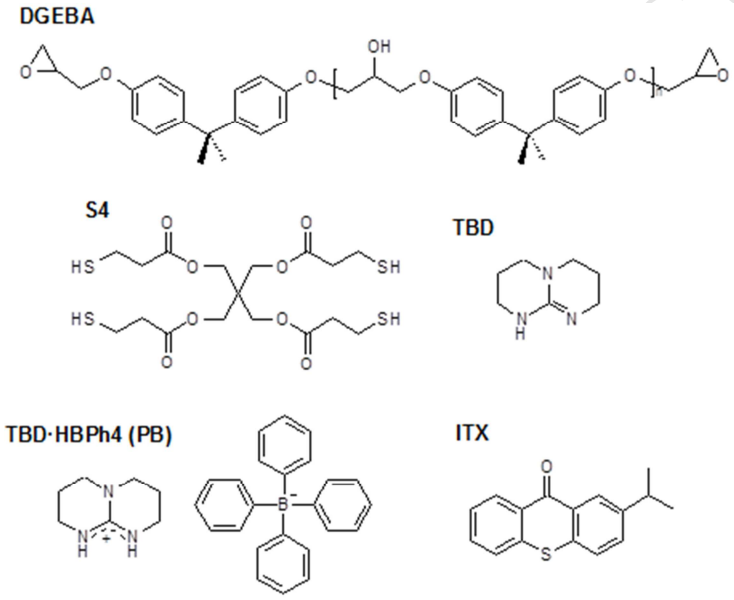

Scheme 2: Structures of the reagents used in this work

2.2 Fourier-transform infrared spectroscopy (FTIR)

We used a Brucker Vertex 70 FTIR spectrometer equipped with an attenuated total reflection (ATR) accessory (GoldenGate™, Specac Ltd.) which is temperature controlled in order to monitor the epoxy-thiol reaction and to verify the degree of cure of the samples. Spectra were collected in absorbance mode with a resolution of 4 cm^{-1} in the wavelength range from 4000 to 600 cm^{-1} averaging 20 scans for each spectrum. Scans were carried out every 60 seconds for a duration of time sufficient to observe the highest achievable conversion.

The absorbance peaks that we used to monitor conversion were 915 cm^{-1} and 2570 cm^{-1} for epoxy and thiol, respectively. These particular wavelengths have inherent complications such as overlaps resulting from the effect of different bonds [7]. As a result, they could only be analyzed qualitatively. We also monitored the hydroxyl band around 3500 cm^{-1} to confirm epoxy consumption.

2.3 Differential Scanning Calorimetry (DSC)

Calorimetric analyses of materials were carried out on a Mettler DSC822e thermal analyzer. UV irradiation of materials were performed on a Mettler DSC821 thermal analyzer using a Hamamatsu LC5 light source equipped with a Hg-Xe mid-pressure lamp conveniently adapted to the DSC by means of fiber optics probes. UV light intensity was approximately 36 mW/cm^2 measured at 365 nm using a radiometer. Both analyzers were calibrated using an indium standard (heat flow calibration). Samples of 4.5 mg (+/- 0.3 mg) were placed in aluminum pans, were irradiated in the DSC821 analyzer, capped with pierced lids and subsequently scanned by DSC822e. Depending on the desired analysis, scans were performed either under isothermal conditions or using temperature ramps of 2.5, 5, 10, or 20ºCmin^{-1} within temperature ranges that completely envelop the curing process. The samples that were to be cured only thermally (i.e. without prior irradiation) were directly analyzed in DSC822e. The fractional conversion x of functional groups and the reaction rate dx/dt are calculated using the following expressions

$$x = \frac{\Delta h}{\Delta h_{total}} \qquad \frac{dx}{dt} = \frac{dh/dt}{\Delta h_{total}} \tag{1}$$

where Δh is the heat released up to a given time/temperature, Δh_{total} is the total reaction heat evolved and dh/dt is the heat flow.

The glass transition temperature T_g of the samples was determined as the halfway point in the heat capacity step during the glass transition, measured by a dynamic DSC scan at 10ºCmin^{-1}. In order to model the dependence of the T_g on the degree of conversion, $T_g(x)$, the expression derived by Venditti and Gillham [18] has been used:

$$ln\, T_g(x) = \frac{(1-x)\cdot ln\, T_{g0} + \lambda \cdot x \cdot ln\, T_{g\infty}}{(1-x) + \lambda \cdot x} \tag{2}$$

$$\lambda = \frac{\Delta C_{p\infty}}{\Delta C_{p0}} \tag{3}$$

Where T_{g0} and $T_{g\infty}$ are the glass transition temperatures (in K) of the uncured and crosslinked materials, and ΔC_{p0} and $\Delta C_{p\infty}$ are the increase in heat capacity during the glass transition of the uncured and crosslinked materials, respectively, measured in the same DSC experiment.

2.4 Curing kinetics

The curing kinetics were analyzed using model-free differential isoconversional methods [19]. The basis for the isoconversional methodology is the expression of the kinetic rate as separable functions of temperature and fractional conversion

$$\frac{dx}{dt} = k(T) f(x) \tag{4}$$

where $k(T)$ is the kinetic constant with an Arrhenius temperature dependence and $f(x)$ is the kinetic model function representing the underlying curing mechanism. For each degree of conversion, it can be shown that the apparent isoconversional activation energy is obtained as

$$\frac{d\ln\left(\frac{dx}{dt}\right)}{d\left(\frac{1}{RT}\right)} = -E \tag{5}$$

The curing kinetics were also analyzed by model-fitting methods. A multiple constant kinetic model [20,21] combining a number of autocatalytic functions with their respective constants was used,

$$\frac{dx}{dt} = f(x,T) = (k_1 + k_1' x^{m_1})(1-x)^{n_1} + \sum_{i=2}^{4} k_i x^{m_i}(1-x)^{n_i} \tag{6}$$

where m_i and n_i are the exponents of each autocatalytic function, and k_i is an Arrhenius kinetic constant for each autocatalytic process. A multi-variate non-linear regression method was used to determine all the kinetic parameters. The results of the kinetics analysis were validated by running simulations using the obtained kinetic parameters and comparing with experimental data. Details of the kinetic modelling can be found in the appendix.

2.5 Storage stability

A set of samples of formulations containing 0.5, 1 and 2phr of PB (i.e. PB05, PB1 and PB2) were prepared in DSC pans and each one was irradiated as per our standard procedure. The samples were placed in a thermostatic bath at 30ºC inside glass tubes filled with silica gel in order to minimize moisture-related effects. To monitor storage stability, PB1 and PB2 samples were analyzed by DSC after 1, 2 and 3 weeks, whereas the PB05 sample was analyzed daily for one week. The stability data for PB05 was later compared with kinetic simulations from the isoconversional differential method. The fractional conversion x of functional groups during storage was determined during the DSC analysis using the following expression

$$x = 1 - \frac{\Delta h_{res}}{\Delta h_{total}} \tag{7}$$

where Δh_{res} is the residual heat released after storage. The T_g of the stored samples was determined in the same DSC experiment. The experimental pairs of x and T_g values were checked with the theoretical $T_g(x)$ relationship obtained from eq. 2.

3 Results and discussion

3.1 Preliminary analysis

We started by investigating the impact of catalyst on epoxy-thiol curing kinetics. In Figure 1, we show the curing profiles of stoichiometric DG187-S4 formulations without catalyst, with 0.5phr PB and UV

irradiated for 15 minutes (*PB05 UV15*), with 0.5phr PB and not irradiated (*PV05 noUV*), and with the equivalent amount of TBD present in *PB05* samples (0.14phr). As can be observed, the uncatalyzed curing started at temperatures above 180 ºC as expected [4]. The onset of curing of *PB05 noUV* was above 150 ºC as liberation of TBD from PB takes place at these temperatures. The slight shoulder at around 170ºC and the broader one at around 200ºC indicate different mechanisms taking effect. The broader one is believed to have occurred due to a purely thermal epoxy-thiol reaction, whereas the earlier might have occured due to secondary activation of PB. Highly stable thiol-epoxy formulations can be prepared using the PB as latent thermal catalyst. The curing profile of *PB05 UV15* was shifted to lower temperatures, owing to the photo-activation of PB to liberate TBD. However, the formulation containing the equivalent amount of TBD cured at much lower temperatures (*TBD014* in Figure 1). In fact, a large amount of heat had already released during sample preparation and thus the DSC scan started at about 25% conversion. A reference value of 405 J/g [3] for the reaction heat was used to determine the conversion of this and the uncatalyzed sample. Measured reaction heats for other samples were acceptably close to the reference value and were thus assumed to be cured completely.

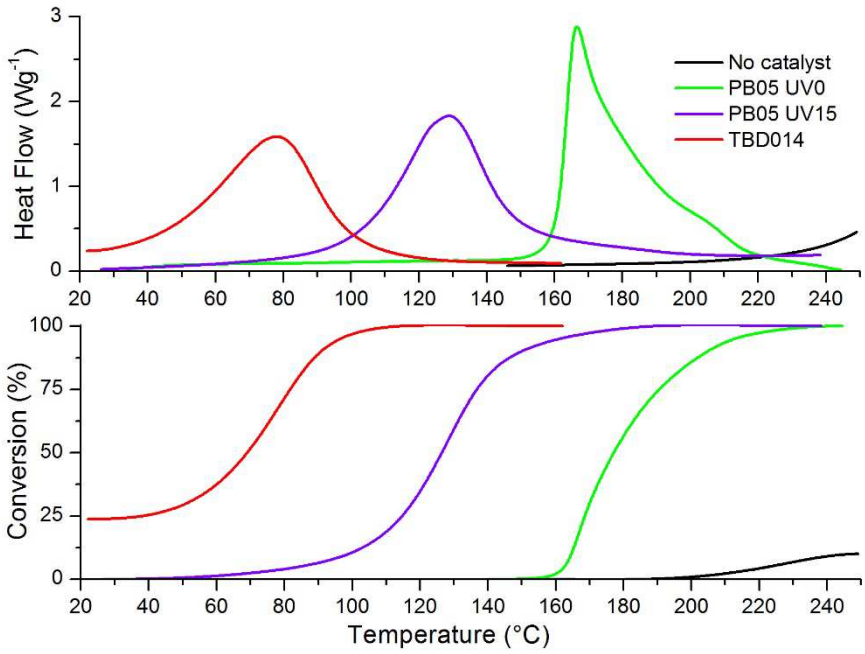

Figure 1: Conversion profiles obtained by DSC for catalyzed and uncatalyzed epoxy-thiol mixtures. All scans were performed using a heating rate of 10ºC/min.

Completion of cure was verified also by FTIR. Figure 2 presents the evolution of FTIR absorption peaks that correspond to thiol, epoxy and hydroxyl groups before and after curing of *PB05 UV15*. One can see the complete disappearance of the thiol peak at 2570 cm^{-1}, accompanied by an appearance of a hydroxyl peak around 3500 cm^{-1}. These indicate total conversion of epoxy groups given the fact that epoxy and thiol groups are in stoichiometry. Due to the overlapping signals around the peak at 915 cm^{-1}, quantitative analysis of epoxy conversion using this peak is impractical. Nevertheless, the decrease of the peak is evident. Similar

results were obtained for *PB05 noUV*, therefore confirming that the curing proceeds via the same reaction mechanism. The T_g of cured samples were within 50-55ºC range which is in aggreement with similar thiol-epoxy formulations after complete cure [22,23].

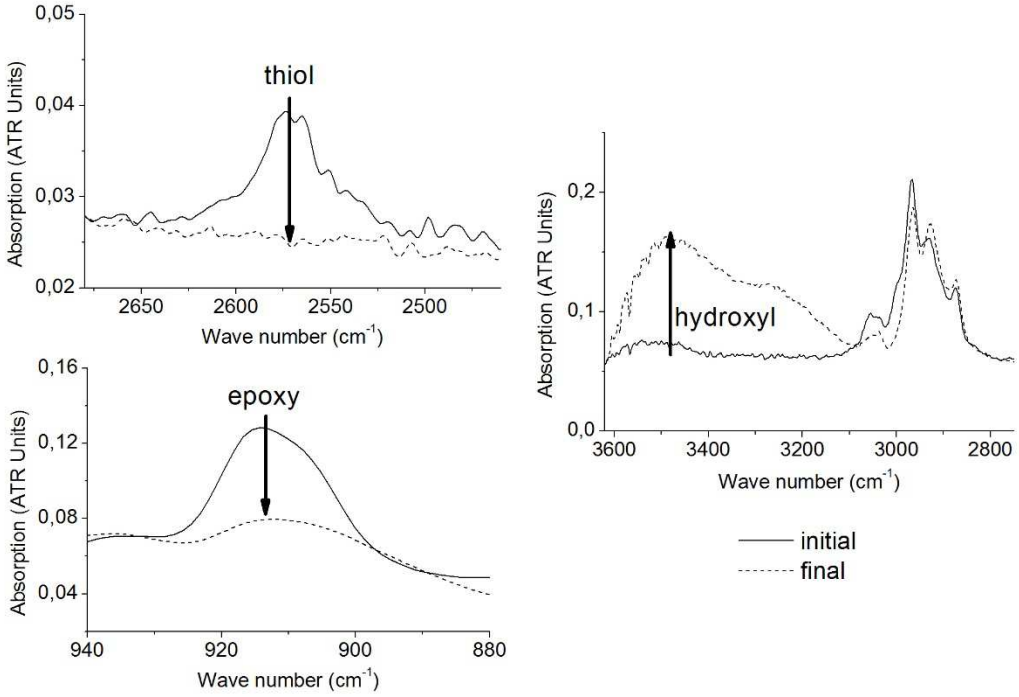

Figure 2:FTIR absorption bands corresponding to different chemical groups for *PB05 UV15* cured at 100°C. The peaks were normalized using the ester absorbance peak at 1720 cm^{-1}.

The results in Figure 1 indicate that the photolysis of the catalyst was incomplete in the *PB05 UV15* sample. This was expected taking into account the low quantum yield of the photolysis of PB [12]. To examine the effect of the irradiation time on the photoactivation of PB, we irradiated samples for different durations and subsequently cured them at 10ºCmin^{-1} in the DSC. As shown in Figure 3, a clear decrease in the curing onset temperature with increasing UV exposure was observed, because of the increased content of TBD released by photolysis. This shows that curing kinetics are governed by not only the pKa of the pristine base, but also its concentration, which increases as UV exposure is continued. Irradiation for longer than 20 minutes enables the curing reaction to commence at near-ambient temperatures, which would be undesirable for applications requiring longer pot-lives. This was not unexpected since Jian et al. [8] and Salmi et al. [11] showed that it was possible to cure thiol-epoxy networks at room temperature by UV-irradiation. Considering these results, we decided that an UV irradiation duration of 15 minutes provides a good balance between stability and reactivity so as to enable separation of the irradiation process from the curing reaction. Consequently, in the rest of the work, UV irradiation durations were fixed at 15 minutes.

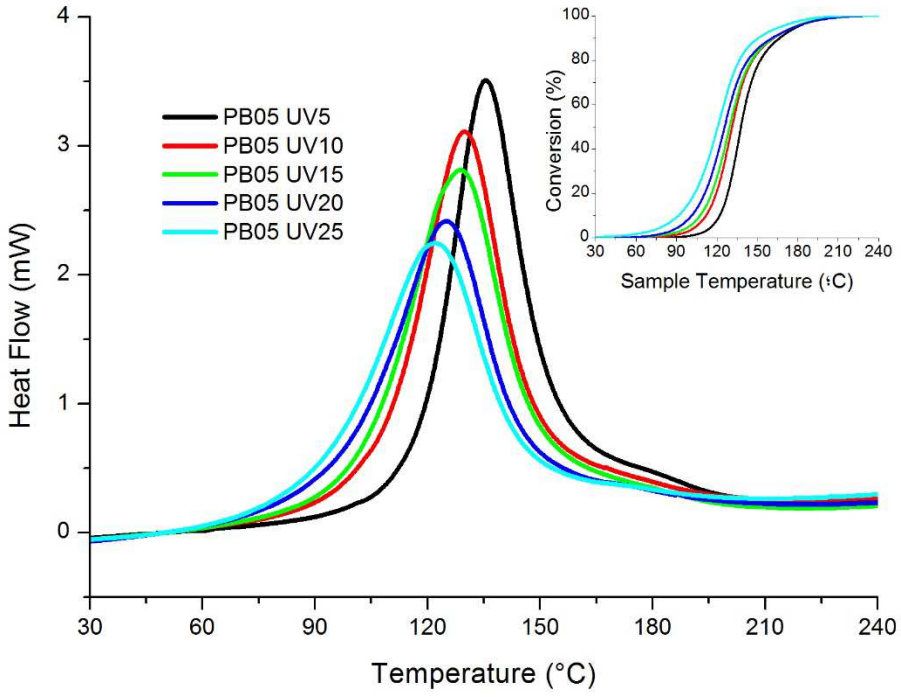

Figure 3: UV irradiation of PB05 sample (which also contains ITX at 0.25phr) for different durations.

We also tested the effect of PB content on the curing profiles of non-irradiated and irradiated samples. Figure 4 compares the dynamic curing at 10 ^{o}Cmin^{-1} of *PB05 noUV*, *PB1 noUV*, and *PB2 noUV* samples.

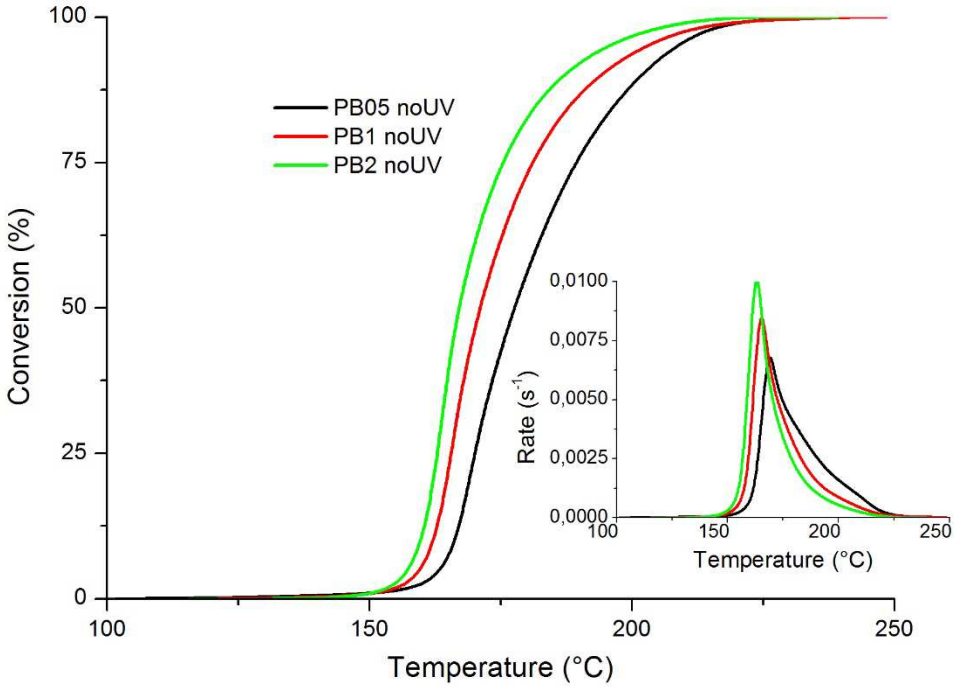

Figure 4: DSC conversion and rate curves of non-irradiated samples with different PB content. Curing was performed at 10 ºC/min.

As can be seen, the thermally activated samples were fairly stable up to 150ºC, regardless of the catalyst concentration. Compared to *PB05 noUV*, note that the maximum reaction rate for *PB2 noUV* was only about 20% greater despite a four-fold increase in catalyst content. Once the catalyst liberates at around 150ºC, the curing reaction follows similar kinetics, independent of PB concentration.

The effect of PB content on the curing of irradiated samples was also tested. Figure 5 compares the dynamic curing of *PB05 UV15* and *PB1 UV15*. Unlike thermally activated samples, curing kinetics of UV activated samples depended heavily on PB concentration. As can be seen, the curing of *PB1 UV15* started at a significantly lower temperature in comparison to that of *PB05 UV15* (approx. 50ºC compared to 100ºC). As reported by other authors, higher PB content and extended irradiation would lead to room-temperature cure in a timely manner [8,11]. We do not report our findings for *PB2 UV15* since UV irradiation for 15 minutes did not suffice to fully activate the PB, as indicated by its DSC thermogram which was disproportional to *PB05 UV15* and *PB1 UV15*. This might have been due to an incomplete dispersion of PB during sample preparation and/or an inefficient penetration of UV light throughout the DSC sample. Note that these factors would have no influence on its thermal decomposition performance. When the stirring of the hot PB-epoxy mixture (during sample preparation), or UV irradiation was continued for longer than 15 minutes, the PB was activated prematurely and the thermal scan failed to capture the curing reaction entirely. These preliminary experiments show that a good balance between reactivity and stability is achieved when a PB concentration of

0.5% (by weight) is used for the DG187-S4 system. As a result, our further kinetics analysis will focus on *PB05* formulations.

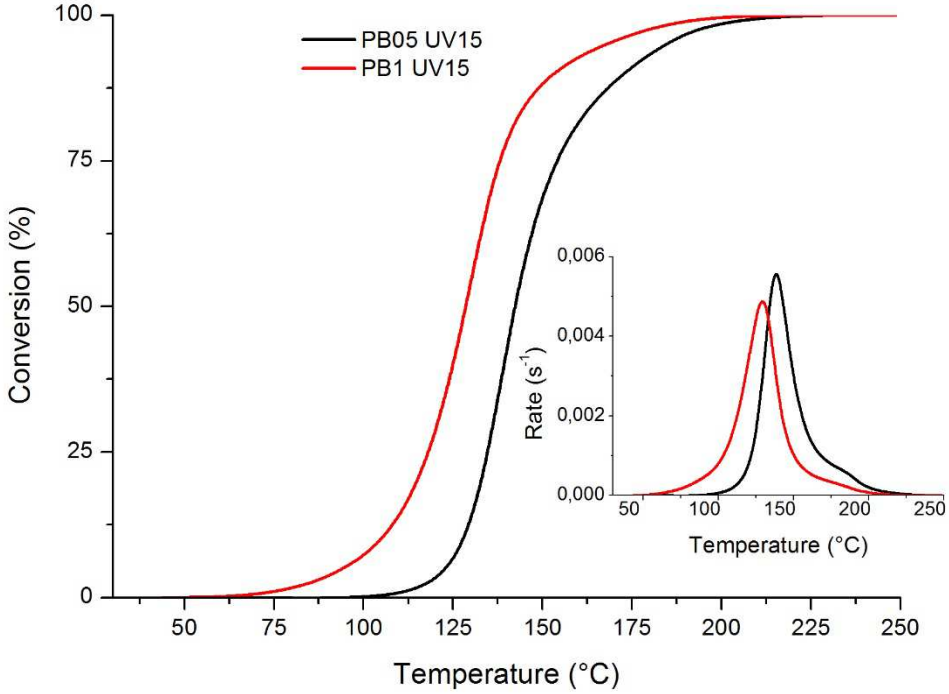

Figure 5: DSC conversion and rate curves for samples with different PB content. Scans were performed at 10 °C/min after UV irradiation for 15 minutes.

Finally, DSC scans were performed to obtain glass transition related parameters of uncured and fully cured samples which will be used to construct the Tg-x relationship using equations 2 and 3. The parameters are given in Table 1.

Table 1. Glass transition temperatures, heat capacity changes, and the λ parameter for uncured and fully cured epoxy-thiol mixtures.

T_{g0}	-33ºC
$T_{g\infty}$	55ºC
ΔC_{p0}	0.512 J.g^{-1}K^{-1}
$\Delta C_{p\infty}$	0.335 J.g^{-1}K^{-1}
λ	0.654

3.2 Kinetic modelling

Figures 6 and 7 show the dynamic and isothermal DSC conversion and rate profiles for samples *PB05 UV15* and *PB05 noUV*, respectively. The dynamic scans hinted the choice of reaction temperatures for the isothermal curing experiments which followed. Heating rates were chosen as 2.5, 5, 10 and 20ºCmin^{-1}. Isothermal temperatures were chosen as 70, 80, 90 and 100ºC for the irradiation scheme, and as 110, 120, 130 and 140ºC for the thermal scheme. As can be verified from Figure 6, irradiated samples cured fairly faster at a given isothermal temperature and the onset temperature was lower in dynamic experiments, at any heating rate. The isothermal thermograms of the irradiated samples have the typical shape of base-catalyzed thiol-epoxy reaction, confirming the autocatalytic behavior of formed hydroxyl groups [4]. In contrast, the non-irradiated samples showed an induction period, shortening with increasing temperature, due to the slow thermal activation of the catalyst and the possible presence of acidic impurities. The overall reaction mechanism is more complex in the thermally activated samples due to the overlapping of thermal decomposition kinetics of PB. In both schemes, the dynamic curing at higher heating rates showed a shoulder extending at higher degrees of conversion and temperatures (See the curves marked as *20ºC/min* in Figures 6 and 7). This suggests there might be secondary processes occurring at elevated temperatures, such as the uncatalyzed thiol-epoxy curing [4]. Also note that the curing rates for *PB05 noUV* at 110ºC and for *PB05 UV15* at 100ºC have matching shapes and peaks with similar orders of magnitude (about 0.05 min^{-1}), suggesting that at similar temperatures, both methods of PB activation yield comparable kinetics, the only difference being the induction period of thermal activation. We verify this observation using simulated kinetic data for *PB05 noUV* at 100ºC. Details of our simulation methods will be presented in the next section.

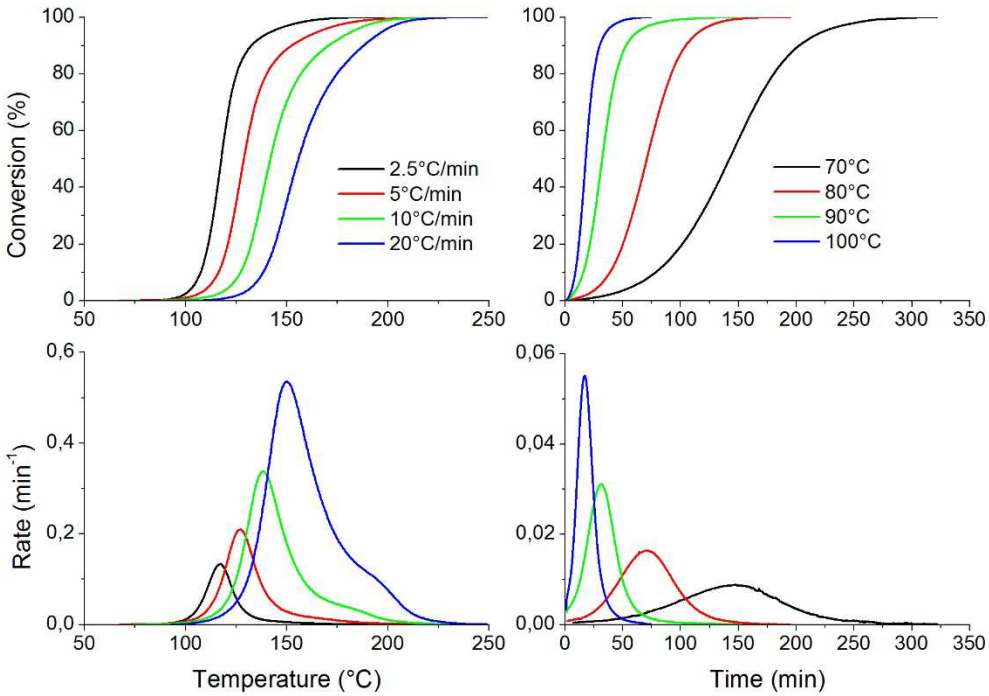

Figure 6: DSC conversion and rate profiles obtained by dynamic and isothermal scans of *PB05 UV15* samples.

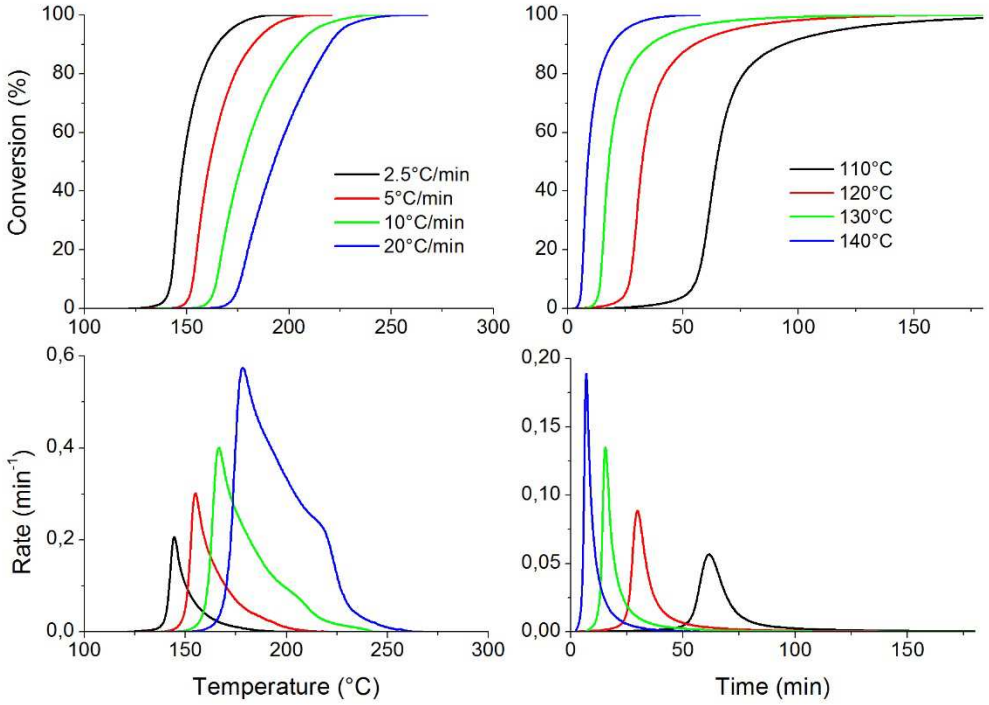

Figure 7: DSC conversion and rate profiles obtained by dynamic and isothermal scans of *PB05 noUV* samples

The differential isoconversional method was applied using 1% conversion steps. Both isothermal and nonisothermal experiments were included in the analysis in order to have a more representative set of results. The analysis was started at 1% of conversion. The performance of the differential method was extremely high as regression coefficients were practically unity throughout the conversion range analyzed. The activation energy profiles of the curing of UV-irradiated and non-irradiated samples are clearly different due to the difference in underlying curing mechanisms. In the thermal process, the thermal decomposition of the initiator takes place at the beginning as the thiol-epoxy condensation kicks off, hence the higher activation energy at the beginning of the process. There could have been thermal decomposition of PB in the UV-irradiated scheme as well due to incomplete activation during UV irradiation. In spite of the complexity of the curing process, we will show later on that the isoconversional kinetic parameters capture appropriately the behavior of the curing system under a wide range of isothermal and nonisothermal conditions.

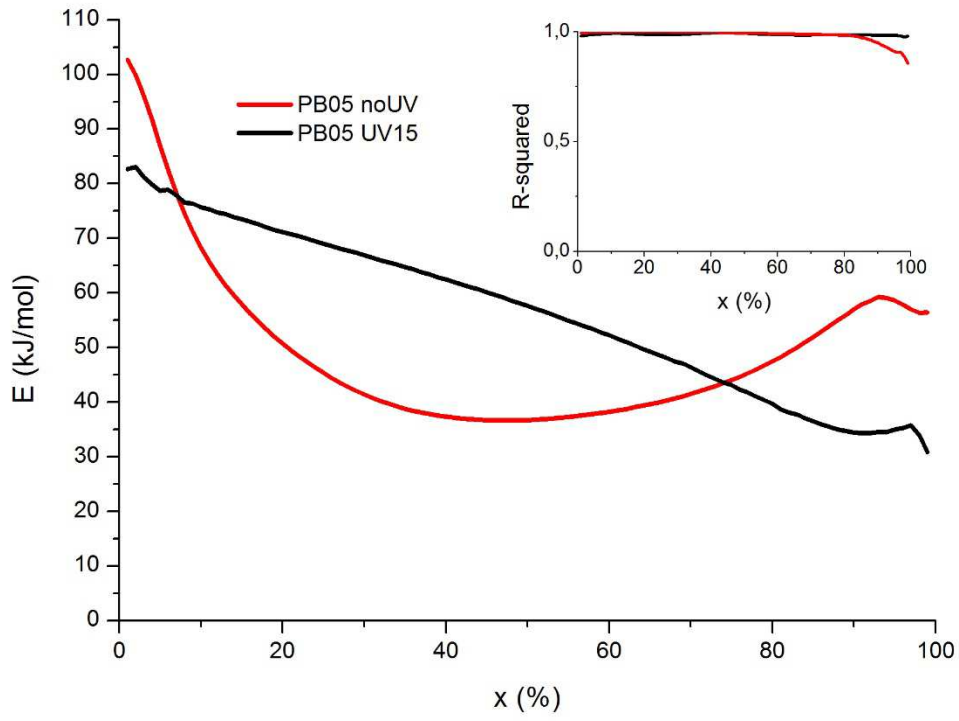

Figure 8: Activation energies and regression coefficients calculated by the isoconversional differential method for epoxy-thiol curing.

The full set of kinetic data was fitted to a multi-term Kamal model by using multi-variate non-linear regression. The conversion range that was included in the fit was 1 to 99% for each dataset. Table 2 summarizes the results of this analysis. As can be seen, functions with different activation energies and reaction orders were obtained reflecting the complexity of the curing process, although it should be noted that the obtained parameters have no physical interpretation. The average error of fitting was 9.7%, which is acceptable considering experimental uncertainties and the fact that a significant number of isothermal and nonisothermal kinetic datasets are fitted to a phenomenological kinetic model. Nevertheless, trends in the

reaction orders and activation energies are in agreement with the isoconversional activation energies, showing that both methods (i.e. isoconversional analysis and Kamal model-fitting) can be used to make curing schedule predictions.

Table 2: Summary of the kinetic parameters obtained from the fitting of the curing kinetics to the isothermal and nonisothermal data.

Term	PB05 noUV				PB05 UV15			
	$E\ (kJ/mol)$	$\ln k_0\ (s)$	m	n	$E\ (kJ/mol)$	$\ln k_0\ (s)$	m	n
1	136.91	27.05	29.46	1.48	150.01	20.00	2.00	3.00
1’	75.58	12.02			101.03	12.67		
2	47.28	10.19	4.15	2.06	130.46	15.48	5.04	2.10
3	32.96	8.07	2.41	4.84	73.91	18.90	1.06	3.24
4	79.55	22.26	1.85	14.14	33.62	5.79	2.81	1.50

The induction period in the thermal scheme is not properly represented by any of the above methods. Formally, the induction period is defined as the time/heating required to reach a fractional conversion of 1%. We determined induction parameters $\ln\left(g(x_{ind})/k_{0,ind}\right) = -24.41\ min$ and $E_{ind} = 88.84\ kJ/mol$ using the methodology described in the appendix. Using these together with the parameters obtained previously in our kinetic analysis, we simulated the isothermal and nonisothermal curing by both isoconversinal and Kamal model fitting methods and compared the results with the experimental data. Figure 9 shows that, in spite of the error of the kinetics analysis, both the model-fitting and the isoconversional analyses capture well the behavior under isothermal and nonisothermal conditions, and at temperatures ranging from 110ºC up to 230ºC. The results also prove the validity for the methodology used for the determination of the induction time-temperature. Minor discrepancies between experimental and simulated are due to the uncertainty in the determination of kinetic parameters and induction time, especially in isothermal experiments at high temperatures.

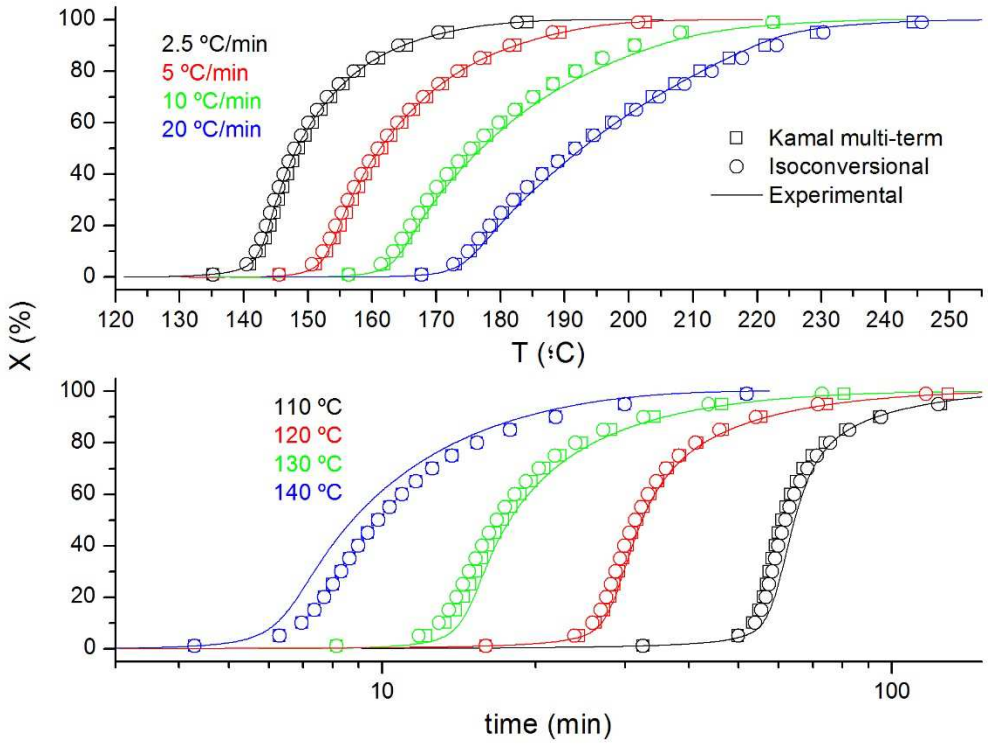

Figure 9: Simulation of the thermally activated epoxy-thiol reaction under nonisothermal and isothermal conditions using the isoconversional and model-fitting kinetic parameters.

Reliable curing schedule predictions can be made at curing temperatures at and above 110ºC. Extrapolation to temperatures below 110ºC might be possible in order to obtain reasonable estimates of low-temperature curing or storage stability. However, the multi-term Kamal model would be more reliable given that the terms of the model equation would change depending on the isothermal curing temperature or the heating program, as one would expect in a complex process. In contrast, the isoconversional simulation assumes the same mechanism regardless of the temperature program.

The kinetics data for irradiated samples were also fitted using the multi-term Kamal model. The fitting parameters are shown in Table 2. Again, the activation energies of the different terms are parallel to the isoconversional activation energies determined previously. The error associated with the analysis was 14% which is higher than that of the thermal activation process. This higher error is due to the further experimental error introduced by irradiating samples of non-uniform thickness and the increased complexity in kinetics due to the thermal activation of the remaining PB. However, the kinetic parameters capture the overall curing behavior (see supporting information) and thus can be used to predict curing schedules even at extrapolated temperatures.

Storage stability is a critical feature of latent curing systems. Not only the curing needs to be activated upon exposure to an external stimulus (i.e. heat or UV light) but also the formulation needs to be sufficiently stable after sample preparation. Extrapolating the results of the kinetic analysis to 30ºC, we estimated,

although with some extrapolation error, an induction period of 3-4 weeks for the *PB05 noUV* sample. In the case of higher PB content, no such latency exists, but a slow curing process reaching completion in a few days. We studied experimentally the storage stability of the *PB05* formulation. Samples of both *PB05 noUV* and *PB05 UV* were kept in a silicone oil thermostatic bath at 30ºC. PB05 noUV was tested weekly for 3 weeks, whereas PB05 UV15 was tested daily until expiry of stability.

The results of the analysis are shown in Figures 10 and 11. It can be seen that *PB05 noUV* was fairly stable up to 3 weeks of storage. Although the simulation predicted an induction period of 3-4 weeks, experiments revealed that no such induction exists possibly due to a slow activation of PB at low temperatures which is not accounted for by the simulation based on kinetic data for higher temperatures. Coupled with the extrapolation error, this could explain the discrepancy. On the other hand, from a practical point of view, a conversion of mere 9% would not be regarded as an expiry in pot-life for most applications.

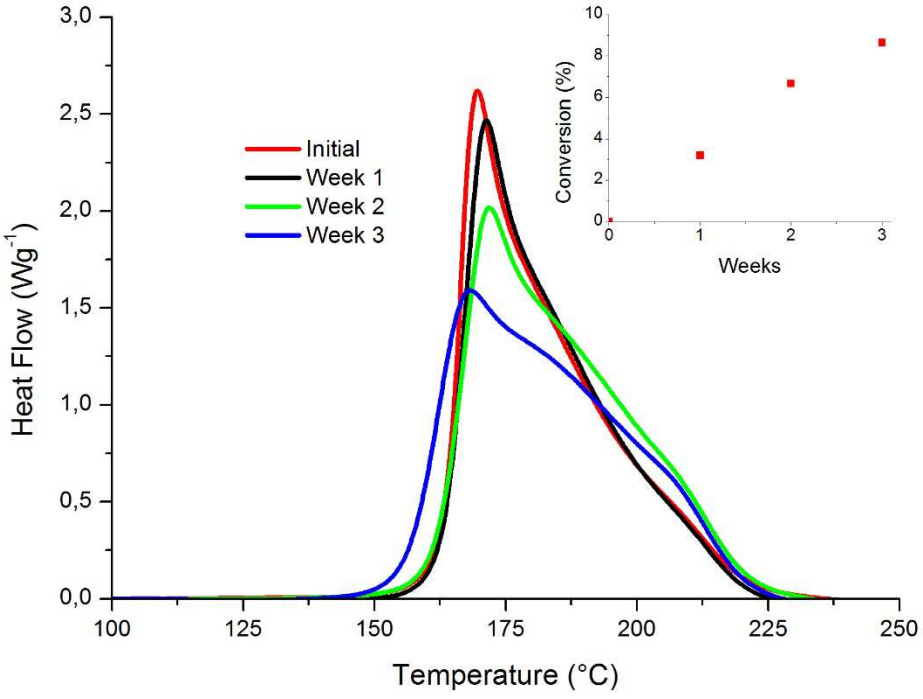

Figure 10: DSC thermograms that show storage stability of PB05 noUV. Scanning rate was 10°C/min.

The results confirm that highly stable formulations could be obtained with PB contents lower than 0.5phr. However, if PB were to be activated only thermally, homogenization at elevated temperatures for product preparation would not be necessary and better storage stability would be possible even with higher PB contents.

We also analyzed the evolution of the *PB05 UV15* samples stored at 30ºC. The results of the analysis are shown in Figure 11 and Table 3 in comparison with predicted curing kinetics and of $T_g(x)$ determined using eq. 2. A good fit between the experimental and predicted kinetics and T_g can be seen. Discrepancies

between experimental and simulated kinetics are due to the fact that samples might contain catalytic impurities which might have effected during storage. These effects are not accounted for in the simulation, therefore a later expiry in storage stability is predicted. However, the time for complete expiry of storage stability is predicted fairly accurately by the simulation. Finally, the T_g-x relationship was represented with high accuracy by the Venditti-Gilham equation as can be seen in Figure 11 (bottom graph). This is another indication of the viability of the curing methodologies employed in this work.

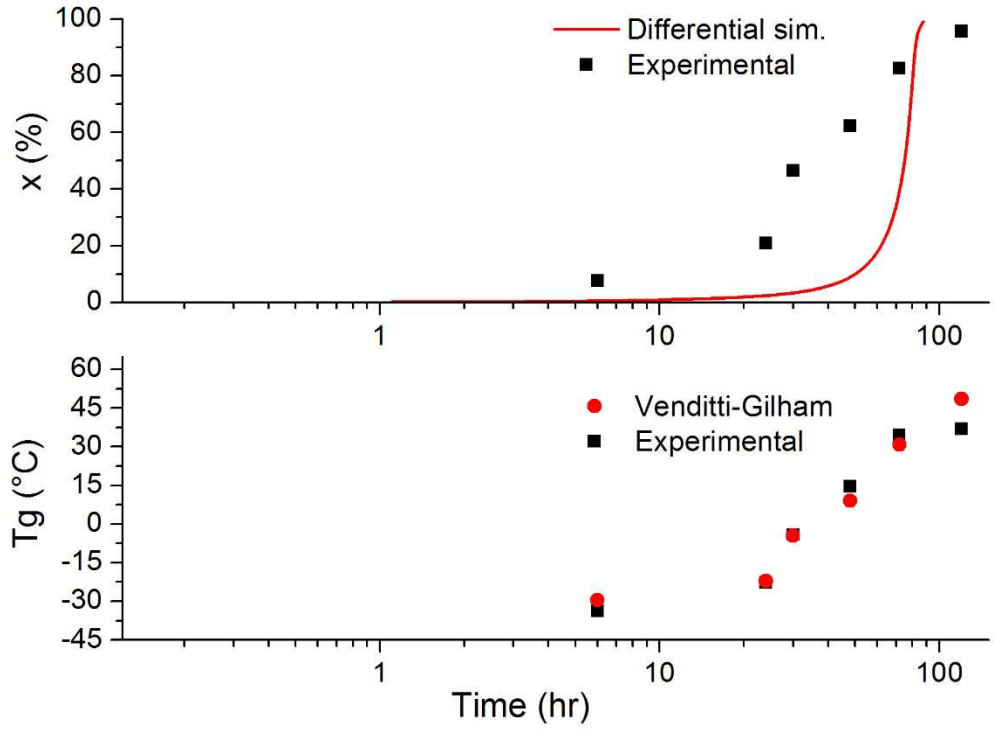

Figure 11: Experimental and predicted fractional degree of conversion and Tg of *PB05 UV15* samples stored at 30°C.

Table 3: Evolution of *PB05 UV15* samples stored at 30°C.

Time (hours)	$\Delta h_{res}\ (J/g)$	x (%)	T_g (ºC)
6	367	8	-34
24	315	21	-23
30	216	47	-4
48	150	62	15
72	69	83	35
120	18	96	37

Both the latency of non-irradiated formulations and the tunable reactivity of irradiated formulations make tetraphenylborate photolatent bases highly promising as catalysts for the preparation of UV-curable or thermally-curable one-pot formulations. A wide range of base-catalyzed reactions could be designed, such as base-catalyzed Michael additions or thiol-click reactions, and also phenol-epoxy, epoxy-anhydride or epoxy-acid reactions. The combination of UV and thermal activation makes tetraphenylborate derivatives useful catalysts for dual-curing formulations such as UV-curable coatings where the thermal activation can make possible complete reaction of the coating in shadowed areas of complex parts [24].

4 Conclusions

The click nature of epoxy-thiol curing reaction allows quantitative yield of the epoxy-thiol thermoset under mild reaction conditions. Base catalysts have been shown to reduce the curing temperature to ambient temperatures which has been verified in this study with TBD. Using a PB such as triazabicyclodecene tetraphenylborate enables the preparation of one-pot formulations that can be stored for several weeks before the final curing process. We showed that the choice of PB activation method (either by UV irradiation or thermally) dictates the reaction onset temperature and as such, could be tailored depending on the storage and/or transportation conditions required. With careful adjustment of PB content and irradiation duration, epoxy-thiol systems could be designed with an optimum balance of reactivity and latency/storage stability. Curing scenarios could be tested with high accuracy using the isoconversional method and the multi-term Kamal model fits demonstrated in this work. The thiol and epoxy monomers used in this study could be combined with other crosslinkable monomers to design versatile dual-curable materials with useful applications in fields such as coatings, adhesives, and composites.

Acknowledgements

The authors would like to thank MINECO (MAT2014-53706-C03-02) and Generalitat de Catalunya (2014-SGR-67 and Serra Húnter programme) for the financial support.

References

[1] Z.W.J. Wicks, F.N. Jones, S.P. Pappas, D.A. Wicks, Organic Coatings - Science and Technology, 3rd ed., John Wiley & Sons, Inc., 2007.

[2] S. De, A. Khan, Efficient synthesis of multifunctional polymers via thiol–epoxy “click” chemistry, Chem. Commun. 48 (2012) 3130. doi:10.1039/c2cc30434a.

[3] D. Guzmán, X. Ramis, X. Fernández-francos, A. Serra, New catalysts for diglycidyl ether of bisphenol A curing based on thiol – epoxy click reaction, Eur. Polym. J. 59 (2014) 377–386. doi:10.1016/j.eurpolymj.2014.08.001.

[4] K. Jin, W.H. Heath, J.M. Torkelson, Kinetics of multifunctional thiol-epoxy click reactions studied by

differential scanning calorimetry: Effects of catalysis and functionality, Polym. (United Kingdom). 81 (2015) 70–78. doi:10.1016/j.polymer.2015.10.068.

[5] J.A. Carioscia, J.W. Stansbury, C.N. Bowman, Evaluation and control of thiol-ene/thiol-epoxy hybrid networks, Polymer (Guildf). 48 (2007) 1526–1532. doi:10.1016/j.polymer.2007.01.044.

[6] R.M. Loureiro, T.C. Amarelo, S.P. Abuin, E.R. Soulé, R.J.J. Williams, Kinetics of the epoxy–thiol click reaction initiated by a tertiary amine: Calorimetric study using monofunctional components, Thermochim. Acta. 616 (2015) 79–86. doi:10.1016/j.tca.2015.08.012.

[7] X. Fernández-Francos, A.-O. Konuray, A. Belmonte, S. De la Flor, À. Serra, X. Ramis, Sequential curing of off-stoichiometric thiol–epoxy thermosets with a custom-tailored structure, Polym. Chem. (2016). doi:10.1039/C6PY00099A.

[8] Y. Jian, Y. He, Y. Sun, H. Yang, W. Yang, J. Nie, Thiol-epoxy/thiol-acrylate hybrid materials synthesized by photopolymerization, J. Mater. Chem. C. 1 (2013) 4481–4489. doi:10.1039/c3tc30360h.

[9] S. Chatani, T. Gong, B.A. Earle, M. Podgorski, C.N. Bowman, Visible-light initiated thiol-Michael addition photopolymerization reactions, ACS Macro Lett. 3 (2014) 315–318. doi:10.1021/mz500132j.

[10] M. Sangermano, A. Vitale, K. Dietliker, Photolatent amines producing a strong base as photocatalyst for the in-situ preparation of organic-inorganic hybrid coatings, Polym. (United Kingdom). 55 (2014) 1628–1635. doi:10.1016/j.polymer.2014.02.045.

[11] H. Salmi, X. Allonas, C. Ley, a. Defoin, a. Ak, Quaternary ammonium salts of phenylglyoxylic acid as photobase generators for thiol-promoted epoxide photopolymerization, Polym. Chem. 5 (2014) 6577–6583. doi:10.1039/C4PY00927D.

[12] X. Sun, J.P. Gao, Z.Y. Wang, Bicyclic guanidinium tetraphenylborate: A photobase generator and a photocatalyst for living anionic ring-opening polymerization and cross-linking of polymeric materials containing ester and hydroxy groups, J. Am. Chem. Soc. 130 (2008) 8130–8131. doi:10.1021/ja802816g.

[13] T. Rodima, I. Kaljurand, A. Pihl, V. Ma, Basicity Scale in THF Solution Ranging from 2-Methoxypyridine to EtP 1 (pyrr) Phosphazene, Society. 1 (2002) 1873–1881.

[14] W.G. Kim, H. Chun, Cure Properties of Naphthalene-Based Epoxy Resin Systems with Hardeners and Latent Catalysts for Semiconductor Packaging Materials, Mol. Cryst. Liq. Cryst. 579 (2013) 39–49. doi:10.1080/15421406.2013.805071.

[15] M.S. Heise, G.C. Martin, J.T. Gotro, Characterization of Imidazole-Cured Epoxy-Phenol Resins, J. Appl. Polym. Sci. 42 (1991) 1557–1566. doi:10.1002/app.1991.070420609.

[16] J. V Crivello, T.P. Lockhart, J.L. Lee, Diaryliodonium salts as thermal initiators of cationic polymerization, J. Polym. Sci. Polym. Chem. Ed. 21 (1983) 97–109. doi:10.1002/pol.1983.170210111.

[17] J. V Crivello, The Discovery and Development of Onium Salt Cationic Photoinitiators, J. Polym. Sci. Part A Polym. Chem. 37 (1999) 4241–4254. doi:10.1002/(SICI)1099-0518(19991201)37:23<4241::AID-POLA1>3.0.CO;2-R.

[18] R. a. Venditti, J.K. Gillham, A relationship between the glass transition temperature (Tg) and fractional conversion for thermosetting systems, J. Appl. Polym. Sci. 64 (1997) 3–14. doi:10.1002/(SICI)1097-4628(19970404)64:1<3::AID-APP1>3.0.CO;2-S.

[19] S. Vyazovkin, N. Sbirrazzuoli, Isoconversional kinetic analysis of thermally stimulated processes in polymers, Macromol. Rapid Commun. 27 (2006) 1515–1532. doi:10.1002/marc.200600404.

[20] N. Boyard, A. Millischer, V. Sobotka, J.-L. Bailleul, D. Delaunay, Behaviour of a moulded composite part: Modelling of dilatometric curve (constant pressure) or pressure (constant volume) with temperature and conversion degree gradients, Compos. Sci. Technol. 67 (2007) 943–954. doi:10.1016/j.compscitech.2006.07.004.

[21] P.I. Karkanas, I.K. Partridge, Cure Modeling and Monitoring of Epoxy / Amine Resin Systems . I. Cure Kinetics Modeling, J. Appl. Polym. Sci. 77 (2000) 1419–1431. doi:10.1002/1097-4628(20000815)77:7<1419::AID-APP3>3.0.CO;2-N.

[22] D. Guzmán, X. Ramis, X. Fernández-Francos, A. Serra, Enhancement in the Glass Transition Temperature in Latent Thiol-Epoxy Click Cured Thermosets, Polymers (Basel). 7 (2015) 680–694. doi:10.3390/polym7040680.

[23] A. Belmonte, D. Guzmán, X. Fernández-Francos, S. De la Flor, Effect of the network structure and programming temperature on the shape-memory response of thiol-epoxy “click” systems, Polymers (Basel). 7 (2015) 2146–2164. doi:10.3390/polym7101505.

[24] C. Decker, F. Masson, R. Schwalm, Dual-curing of waterborne urethane-acrylate coatings by UV and thermal processing, Macromol. Mater. Eng. 288 (2003) 17–28. doi:10.1002/mame.200290029.

[25] M.J. Starink, The determination of activation energy from linear heating rate experiments: A comparison of the accuracy of isoconversion methods, Thermochim. Acta. 404 (2003) 163–176. doi:10.1016/S0040-6031(03)00144-8.

[26] X. Fernández-Francos, A. Rybak, R. Sekula, X. Ramis, A. Serra, Modification of epoxy-anhydride thermosets using a hyperbranched poly(ester-amide): I. Kinetic study, Polym. Int. 61 (2012) 1710–1725. doi:10.1002/pi.4259.

[27] E. Ruiz, F. Trochu, Numerical analysis of cure temperature and internal stresses in thin and thick RTM

parts, Compos. Part A Appl. Sci. Manuf. 36 (2005) 806–826. doi:10.1016/j.compositesa.2004.10.021.

[28] S. Vyazovkin, Evaluation of Activation Energy of Thermally Stimulated Solid-State Reactions under Arbitrary Variation of Temperature, J. Comput. Chem. 18 (1997) 393–402. doi:10.1002/(SICI)1096-987X(199702)18:3<393::AID-JCC9>3.0.CO;2-P.

[29] L.A. Pérez-Maqueda, J.M. Criado, Accuracy of Senum and Yang's approximations to the Arrhenius integral, J. Therm. Anal. Calorim. 60 (2000) 909–915. doi:10.1023/A:1010115926340.

Appendix

A. Differential isoconversional method

The curing kinetics were analyzed by isoconversional methods [19]. The basic assumption of all isoconversional methods is that the rate of a reaction can be expressed as a product of two separable functions of the fractional degree of conversion x and the curing temperature T,

$$\frac{dx}{dt} = k(T)f(x) \tag{A.1}$$

where $f(x)$ is the kinetic model function representing the underlying curing mechanism and $k(T)$ is the Arrhenius kinetic constant given as follows

$$k = k_0 \exp(-\frac{E}{RT}) \tag{A.2}$$

where k_0 is the pre-exponential factor of the rate constant, E is the activation energy, and R is the universal gas constant.

To be able to use equation (A.1), one would need to know the function $f(x)$, and the constants k_0 and E. However, in model-free isoconversional methods the elucidation of the kinetic model $f(x)$ is not necessary. The differential isconversional method used in this work, also known as Friedman method [19,25] based on the linear expression obtained from the combination of equations (A.1) and (A.2) and taking the natural logarithm of both sides.

$$\ln\left(\frac{dx}{dt}\right) = ln[k_0 f(x)] - \frac{E}{RT} \tag{A.3}$$

For each degree of conversion, it can be shown that the apparent isoconversional activation energy is obtained as

$$\frac{d\ln\left(\frac{dx}{dt}\right)}{d\left(\frac{1}{RT}\right)} = -E \tag{A.4}$$

Therefore, from eq. A.3, a plot of $\ln(dx/dt)$ versus $1/RT$ at a given conversion from experiments at different heating rates or isothermal temperatures will be a line with slope $-E$ and y-intercept $ln[k_0 f(x)]$. This analysis is usually carried out within all the conversion range at discrete and regular conversion steps of 1-2%, so that pairs of E and $ln[k_0 f(x)]$ values are obtained for each degree of conversion. These kinetic parameters can be used to simulate curing processes with random temperature programs by numerical integration of eq. A.1. A value at 0 % conversion can be extrapolated for subsequent simulation but this might lead to errors in situations where there is a significant induction period e.g. due to the slow activation of a latent catalyst.

B. Model fitting methodology

The kinetics have also been analyzed by model-fitting methods. A popular model that can be used for the analysis of the curing kinetics various thermosetting systems, including the thiol-epoxy reaction, is the Kamal model [4,26] shown in eq. A.5.

$$\frac{dx}{dt} = (k_1 + k_2 x^m)(1-x)^n \tag{A.5}$$

However, some epoxy systems cure through complex reaction steps, therefore one should use a modified and more complex model to account for the contribution of these different reaction steps. In this work we have used a multi-term Kamal model inspired in the models employed by other authors [20,21] shown in eq. A.6,

$$\frac{dx}{dt} = f(x,T) = (k_1 + k_1' x^{m_1})(1-x)^{n_1} + \sum_{i=2}^{4} k_i x^{m_i}(1-x)^{n_i} \tag{A.6}$$

where m_i and n_i are the exponents of each autocatalytic function, and k_i is an Arrhenius kinetic constant for each autocatalytic process. Although one can use a higher number of terms for the Kamal model as an attempt to increase goodness of fit, we saw that no significant improvement is achieved with more than 4 terms. The number of adjustable parameters is high, as it includes E_i and $k_{0,i}$ for the different k_is and the reaction orders m_i and n_i for each autocatalytic function. We used GRG Nonlinear Solving method (Microsoft Excel) to minimize the average relative error which is given by the following equation.

$$error = \frac{1}{n}\sum \frac{\left|\left(\frac{dx}{dt}\right)_{exp} - \left(\frac{dx}{dt}\right)_{calc}\right|}{\left(\frac{dx}{dt}\right)_{calc}} \tag{A.7}$$

where $(dx/dt)_{exp}$ and $(dx/dt)_{exp}$ are the experimentally measured, and the calculated reaction rates, respectively, at the same degree of conversion, and n are the number of calculated and measured points used for the fitting. Given that the fitting is performed on reaction rate with respect to conversion rather than on conversion with respect to temperature/time, the effect of an induction period i.e. due to the slow activation of a latent catalyst might not be properly accounted for.

C. Determination of the induction period

One can define an induction time t_{ind} as the time to reach a given conversion, x_{ind}, using the following expression based on the integration of the rate equation [19] and assuming the validity of isoconversional hypotheses during the induction period.

$$g(x_{ind}) = \int_0^{x_{ind}} \frac{dx}{f(x)} = k_{0,ind} \cdot \int_0^{t_{ind}} \exp\left(-\frac{E_{ind}}{R} \cdot \frac{1}{T}\right) \cdot dt \qquad \text{(A.8)}$$

Where $g(x_{ind})$ is the integral form of the kinetic model function $f(x)$ at the induction fractional conversion x_{ind}, and E_{ind} is the activation energy corresponding to the induction period. The parameters $\ln\left(g(x_{ind})/k_{0,ind}\right)$ and E_{ind} are assumed to be constant during the induction period, and are determined by numerical integration and nonlinear regression of the above expression for a number of experiments under arbitrary temperature programs. The use of eq. A.8 is implicit in the methods used by other authors [27].

Under isothermal conditions, a more simplified version of eq. A.8 can be used

$$\ln t_{ind} = \ln\left(\frac{g(x_{ind})}{k_{0,ind}}\right) + \frac{E_{ind}}{R} \cdot \frac{1}{T} \qquad \text{(A.9)}$$

where it can be seen that the parameters are obtained simply by regression of $\ln t_{ind}$ with respect to T^{-1} under different isothermal conditions.

Under constant heating rate experiments, one can make use of the approximation of the temperature integral as:

$$\frac{g(x_{ind})}{k_{0,ind}} = \frac{1}{\beta} \cdot \frac{E_{ind}}{R} \cdot p(y) \qquad \text{(A.10)}$$

where β is the heating rate, $y = E_{ind}/R \cdot T_{ind}$, T_{ind} is the temperature at the defined induction fractional conversion, and $p(y)$ is an approximation of the temperature integral, for instance the Senum-Yang approximation [28,29].

A determination of $\ln\left(g(x_{ind})/k_{0,ind}\right)$ and E_{ind} from both isothermal and constant heating rate experiments can therefore be made by nonlinear regression techniques, making use of simplified expressions A.9 for isothermal experiments and A.10 for dynamic experiments, rather than numerical integration of A.8. Likewise, the induction time for isothermal temperatures or constant heating rates can be determined making use of the same expressions. Once the induction period is over, the simulation can be carried out either using eq. A.1 starting from x_{ind} and the isoconversional pairs of E and $ln[k_0 f(x)]$ values obtained from the differential isoconversional analysis. Or else the simulation can be performed by numerical integration of eq. A.6. using the adjusted parameters. The choice of x_{ind} may be somewhat arbitrary and depend on the shape of the conversion curves and the accuracy of the experimental data.

LATENT CURING OF EPOXY-THIOL THERMOSETS

HIGHLIGHTS

- Photobase can be activated by UV light or heat to start epoxy-thiol curing
- Curing at near-ambient conditions is possible with UV activation
- Several weeks of pot-life is achievable without compromising good curing rates
- Curing kinetics are comparable regardless of photobase activation method